Evidence for site-specific strong and weak pinning of the modulation wave in the incommensurate phases of randomly quenched Rb_2ZnCl_4 systems

1999 J. Phys.: Condens. Matter 11 5065

(http://iopscience.iop.org/0953-8984/11/26/309)

J. Phys.: Condens. Matter **11** (1999) 5065–5082. Printed in the UK PII: S0953-8984(99)00433-6

Evidence for site-specific strong and weak pinning of the modulation wave in the incommensurate phases of randomly quenched Rb_2ZnCl_4 systems

S Uma Maheswari, K Venu and V S S Sastry

School of Physics, University of Hyderabad, Hyderabad-500 046, India

E-mail: vssssp@uohyd.ernet.in

Received 29 December 1998

Abstract. The influence of randomly quenched disorder in the incommensurate phases of $Rb_2(Zn_{1-x}Cu_x)Cl_4$ (for $x = 0.03$), $Rb_2(Zn_{1-x}Cd_x)Cl_4$ (for $x = 0.03$ and 0.05), $Rb_2(Zn_{1-x}Hg_x)Cl_4$ (for $x = 0.03$ and 0.05) and $Rb_2Zn(Cl_{1-x}Br_x)_4$ (for $x = 0.01$ and 0.03) is investigated via the amplitudon and phason dynamics using ^{35}Cl nuclear quadrupole resonance studies. Defect pinning at the metal and halogen sites in the prototype compound Rb_2ZnCl_4 has been attempted for the first time and has yielded novel results. Quenched randomness at the metal site (Zn) in Rb_2ZnCl_4 induced strong pinning of the modulation wave (irrespective of the size of the dopant compared to the host). This is evident from a temperature-independent Δ_ϕ and consequently $T_{1\phi}$ unlike the case for impurity pinning at the other sites (cation and anion). The effect is enhanced with increasing concentration of the dopant. This result is contrasted with defect pinning at the halogen site (Cl) in Rb_2ZnCl_4 with Br substitution which induced weak pinning of the modulation wave (temperature-dependent Δ_ϕ and consequently $T_{1\phi}$) similarly to substitution at the cation site as seen from earlier studies. Furthermore, the impurities have been categorized as *random-field* or *random-potential* type by evaluating the symmetry parameter (m) associated with the impurity. It is seen that Cu, Cd and Hg are *random-field*-type impurities inducing strong pinning of the modulation wave ($m < 6$; $m = 6$ for Rb_2ZnCl_4) while the Br impurity is of a *random-potential* type inducing a weak pinning of the modulation wave.

1. Introduction

The order parameter excitation spectrum of incommensurate systems consists of an acoustic-like phason branch and an optic-like amplitudon branch. According to the continuum theory in the plane-wave limit (PWL) [1], the phason is gapless in the absence of any pinning and represents the Goldstone mode recovering the broken translational symmetry (of the free energy) of the incommensurate (IC) phase. Development of incommensurate order with decreasing temperature in this phase leads to the breakdown of the plane-wave approximation and the realization of phase solitons (domain walls separating essentially commensurate regions) [2, 3]. The discrete nature and defects of the lattice, as well as the presence of quenched disorder, could have profound effects on the development of the multi-soliton lattice close to the lock-in transition [2, 3]. Any phase-pinning perturbation will introduce a gap in the phason spectrum, and defects are expected to have a strong influence on the pinning scenario.

0953-8984/99/265065+18$19.50

The symmetry properties of the dopant are known to play an important role in determining the properties of the incommensurate phase [4]. In this context, doping of Rb_2ZnCl_4 at the cation site with symmetry-non-breaking ions (like K) [5] smaller in size compared to the host cation have only a subtle effect on the transition temperature T_I, while in the presence of a heavier cation (Cs) both T_I and T_C are considerably suppressed, with the effect being enhanced with increasing impurity concentration [6]. On the other hand, doping studies with symmetry-breaking ions have been very scarce on the otherwise widely investigated compound Rb_2ZnCl_4. ^{35}Cl NQR studies on NH_4^+ doping at the cation site in Rb_2ZnCl_4 have been reported [7–9]; the doping suppressed T_C considerably and induced Devil's staircase behaviour in the multi-soliton limit. Studies of the incommensurate phase with doping at the metal and halogen sites in Rb_2ZnCl_4 have not been attempted so far to the best of our knowledge. Such a study has been taken up in the present work to investigate the effect of the site of occupation and size of the dopant in Rb_2ZnCl_4 so as to allow us to compare the results with those for the doping of cations of different sizes in the same system [8, 10, 11]. It was reported earlier in an x-ray study on the A_2ZnCl_4 systems [12] that substitution at the metal site distorts the basic tetrahedron ($ZnCl_4$) itself. As the geometry of the tetrahedron ($ZnCl_4$) influences the onset of a transition to the incommensurate phase [13], it could lead to very specific and interesting effects. Also the rotational dynamics of the anion is known to be crucially involved in mediating the paraelectric–incommensurate transition in Rb_2ZnCl_4 [14]. The geometry of the $(ZnCl_4)^{2-}$ anions being perturbed by substitution at the halogen site in the present work could perhaps lead to interesting results regarding the dynamic processes in the incommensurate phase. In this context, Br substitution at the Cl site in Rb_2ZnCl_4 has been attempted here, along with doping of Cu, Cd and Hg (at various concentrations) at the Zn site in Rb_2ZnCl_4.

2. Experimental details

$Rb_2(Zn_{1-x}Cu_x)Cl_4$ (for $x = 0.03$), $Rb_2(Zn_{1-x}Cd_x)Cl_4$ (for $x = 0.03$ and 0.05), $Rb_2(Zn_{1-x}Hg_x)Cl_4$ (for $x = 0.03$ and 0.05) and $Rb_2Zn(Cl_{1-x}Br_x)_4$ (for $x = 0.01$ and 0.03) are grown by the slow evaporation of stoichiometrically prepared aqueous solutions. Doubly recrystallized polycrystalline samples are used. Of the three ^{35}Cl NQR lines observed for all of the samples in the high-temperature paraelectric phase, the line corresponding to the highest frequency (ν_1) can be most conveniently tracked into the incommensurate phase, as it is broadened by about 100 kHz as compared to the broadening of about 500 kHz of the other two lines, making their observation difficult. Hence all measurements are carried out on the high-frequency line (ν_1). For all of the compounds, below T_I, three singularities (ν_+, ν_- and ν_ϕ) of the otherwise inhomogeneously broadened NQR line are observed throughout the incommensurate phase. Measurements on the temperature dependence of the singularities (ν_+, ν_- and ν_ϕ) are carried out applying narrow-band excitations of the different spin packets by applying longer rf pulse widths (typically a $\pi/2$ pulse width is about 80 μs). For recording the singularities in the incommensurate phase, the excitation frequency is increased in steps of 2 kHz over a band of 100 kHz on either side of the extrapolated high-temperature frequency, with averaging carried out over 1024 acquisitions. While a spin echo is used to locate the singularities, an inversion-recovery spin-echo sequence (π–τ–$\pi/2$–τ'–π; $\tau' = 180$ μs) is used to measure the quadrupolar spin–lattice relaxation times (T_{1Q}). The accuracy in the measurement of the frequency is within $\pm$1.5 kHz, while it is within 5% for T_{1Q}. A gas-flow-type cryostat with liquid nitrogen vapour is used for temperature variation with a stability of $\pm$0.5 K over two hours.

3. Theory

NQR spectroscopy is perhaps the most extensively used technique for studying phase transitions in structurally incommensurate phases as the resonance frequency varies in space reflecting the spatial variation of the incommensurate modulation. In incommensurate systems there are essentially an infinite number of non-equivalent nuclear sites that contribute to the resonance spectrum, resulting in a quasi-continuous distribution of the resonance frequency [1]. Due to this modulation there is a bunching of spins on the frequency axis giving rise to singularities on the resonance line.

3.1. The NQR line shape

Considering the modulation in the plane-wave limit (PWL, when the phase of the modulation is a linear function of the displacement) and the local case: when the wavelength of the incommensurate modulation is large compared to the region from which the dominant contribution to the NQR frequency arises, the resonance frequency ν at a given lattice site can be expanded in a power series in the displacement field u [15, 16] as

$$\nu = \nu_0 + a_1 u + \frac{1}{2} a_2 u^2 + \cdots \tag{1}$$

where ν_0 is the NQR frequency at the transition temperature T_I and $u = A\cos\phi(x)$, where A is the order parameter for the paraelectric–incommensurate transition and ϕ is the phase of the incommensurate modulation wave. Thus,

$$\nu = \nu_0 + \nu_1 \cos\phi + \frac{1}{2}\nu_2 \cos^2\phi + \cdots \tag{2}$$

where $\nu_1 \propto A$ and $\nu_2 \propto A^2$ etc. In the incommensurate phase, $\cos\phi$ takes continuously all values from +1 to −1. The frequency distribution in the plane-wave limit is defined as [16]

$$f(\nu) = \frac{\text{constant}}{\mathrm{d}\nu/\mathrm{d}\phi}. \tag{3}$$

The spectral density $f(\nu)$, which is an inhomogeneous line shape, will be peaked or have singularities whenever $\mathrm{d}\nu/\mathrm{d}\phi \to 0$. If the site symmetry of the nucleus in the high-temperature phase is such that the linear and quadratic terms in equation (2) are taken into account, three distinct singularities are obtained when $|\nu_1| \leqslant |\nu_2|$. The edge singularities corresponding to maximum displacement of the modulation wave ($\cos\phi = \pm 1$) will arise at [1, 16]

$$\nu_\pm = \nu_0 \pm \nu_1 + \frac{1}{2}\nu_2 \tag{4}$$

while the other singularity corresponding to $\nu_1 + \nu_2 \cos\phi = 0$ will arise at

$$\nu_\phi = \nu_0 - \frac{\nu_1^2}{2\nu_2}. \tag{5}$$

Furthermore, the frequency and width of ν_ϕ will be independent of temperature while the edge singularities will be temperature dependent. The ν_ϕ-singularity arises due to the non-linearity in the relation between the resonance frequency and the order parameter. The splitting between the edge singularities at any temperature T is given by [1, 16]

$$\Delta\nu = \nu_+ - \nu_- = 2\nu_1 \propto A \propto (T_I - T)^\beta \tag{6}$$

where β is the critical exponent associated with the order parameter characterizing the transition.

3.2. Nuclear spin–lattice relaxation

Since the energy of the incommensurate phase in the continuum limit is independent of the phase of the incommensurate modulation wave, these systems have phason branches which dominate the relaxation mechanisms [1]. In contrast to the case for periodic systems, the spin–lattice relaxation time (T_{1Q}) will vary over the inhomogeneously broadened NQR line and allow for a separate estimation of the phason and amplitudon contributions [1, 16]. The spin transition probabilities, $W^{(\mu)}$, for the lth nucleus due to the amplitudon and phason excitations in the 'local' approximation [16] and mediated via direct one-phason and one-amplitudon relaxation processes are given by [1]

$$W^{(\mu)} = \text{constant} \times \left[\cos^2\phi(x_l)\, J_A^{(\mu)}(\omega) + \sin^2\phi(x_l)\, J_\phi^{(\mu)}(\omega)\right] \tag{7}$$

where $J_A^{(\mu)}$ and $J_\phi^{(\mu)}$ are the local spectral densities of the auto-correlation functions of the amplitudon and phason fluctuations, respectively. In the PWL, $J_\phi^{(\mu)}$ is found to be temperature independent in the high-temperature part of the incommensurate phase in Rb_2ZnCl_4, whereas $J_A^{(\mu)}$ decreases with decreasing temperature [17]. Amplitudons will dominate relaxation for nuclear sites where $\cos^2\phi(x_l) = 1$ and hence at the edges of the spectrum. The phasons will dominate the relaxation for nuclear sites with $\cos^2\phi(x_l) = 0$, and hence in the centre of the spectrum. From the transition probabilities, the amplitudon and phason contributions to the relaxation rates, $(T_{1A})^{-1}$ and $(T_{1\phi})^{-1}$ respectively, can be evaluated. The effective spin–lattice relaxation rate over the inhomogeneous frequency distribution for direct processes can be written as

$$T_1^{-1} = X^2 T_{1A}^{-1} + (1 - X^2) T_{1\phi}^{-1} \tag{8}$$

where $X = \cos\phi$.

3.3. The phason gap

In the PWL, the phason branch has an acoustic-like dispersion and is gapless in the absence of pinning. Any pinning of the modulation wave to the underlying lattice due to the presence of discrete-lattice effects or the presence of impurities will introduce a gap Δ_ϕ in the phason spectrum as [1, 16]

$$\omega_\phi^2 = \Delta_\phi^2 + Kk^2 \tag{9}$$

where ω_ϕ is the phason frequency and k is the wave vector associated with the modulation wave. Relaxation measurements directly give an estimate of the phason gap Δ_ϕ from a known amplitudon gap Δ_A [18]. For direct one-phonon processes in the plane-wave regime, large frequency-dependent phason- and amplitudon-induced spin–lattice relaxation rates are given by [1]

$$T_{1\phi}^{-1} = C\frac{\pi}{4}k^{-3/2}\frac{\Gamma_\phi}{\Delta_\phi} \tag{10}$$

$$T_{1A}^{-1} = C\frac{\pi}{4}k^{-3/2}\frac{\Gamma_A}{\Delta_A} \tag{11}$$

where C is a constant proportional to the square of the fluctuating EFG tensor, and Γ_ϕ and Γ_A are the phason and amplitudon damping constants, respectively. In the mean-field approximation, Δ_A represents the temperature-dependent energy gap in the amplitudon spectrum and is given by [16]

$$\Delta_A \propto K_2\sqrt{T_I - T}. \tag{12}$$

Here, Δ_A is of the order of a phonon frequency at temperatures different from T_I, and since $\Gamma_\phi = \Gamma_A = \Gamma$ and $\omega_Q \ll \Gamma \ll \Delta_A$, the relaxation times due to the amplitudon and phason fluctuations can be written as

$$\frac{T_{1\phi}}{T_{1A}} = \frac{\Delta_\phi}{\Delta_A}. \tag{13}$$

Thus the measurement of $T_{1\phi}$ and T_{1A} in the incommensurate phase allows for a determination of the phason gap Δ_ϕ in terms of a known amplitudon gap Δ_A. The temperature dependence of Δ_A can be obtained by fitting the corresponding relaxation time data to

$$T_{1A} = K_1\Delta_A \propto K_1K_2\sqrt{(T_I - T)}. \tag{14}$$

From the neutron scattering measurements for Rb_2ZnCl_4, the amplitudon gap was estimated to be 0.256×10^{12} s^{-1} [19] which corresponds to a T_{1A}-value of 15 ms [8]. Using these values, K_1 was found to be 58.594×10^{-12} s^2. The temperature dependence of the amplitudon gap in the various compounds investigated here is calculated from equation (14) and that of the phason gap from equation (13).

4. Results

Three singularities (ν_+, ν_- and ν_ϕ) are observed in all of the compounds with doping at the metal site ($Rb_2(Zn_{1-x}B_x)Cl_4$; B $\equiv$ Cu for $x = 0.03$, Cd for $x = 0.03$ and 0.05 and Hg for $x = 0.03$ and 0.05) and at the halogen site i.e., in $Rb_2Zn(Cl_{1-x}Br_x)_4$ for $x = 0.01$ and 0.03, as in the pure Rb_2ZnCl_4 sample. The separation between the singularities increases with decreasing temperature as expected from equation (6). The temperature variations of the singularities in the above compounds are shown in figures 1 to 7 respectively. The solid curves in these figures show the fit of the data to $\Delta\nu \propto (T_I - T)^\beta$. The values of the critical exponent β so obtained from the fits is 0.35 ± 0.01 for all of these compounds (table 1) and is the same as for the pure compound ($\approx$0.35) indicating that the critical behaviour of the modulation wave

Table 1. Variation of transition temperatures (T_I and T_C), critical exponent (β), phason gap $\Delta_{\phi c}$ at T_C and the symmetry parameter (m) with impurity doping.

Compound	T_I (K)	T_C (K)	β	$\Delta_{\phi c}$ (10^{11} s^{-1})	m
Rb_2ZnCl_4	302	192	0.34	0.21	6
$Rb_2(Zn_{1-x}Cu_x)Cl_4$					
$x = 0.03$	303	190	0.34	0.42	5
$Rb_2(Zn_{1-x}Cd_x)Cl_4$					
$x = 0.03$	305	185	0.34	0.61	4
$x = 0.05$	308	180	0.34	0.90	
$Rb_2(Zn_{1-x}Hg_x)Cl_4$					
$x = 0.03$	305	184	0.34	0.60	4
$x = 0.05$	308	180	0.34	0.91	
$Rb_2Zn(Cl_{1-x}Br_x)_4$					
$x = 0.01$	300	188	0.35	0.80	6
$x = 0.03$	293	180	0.35	1.04	

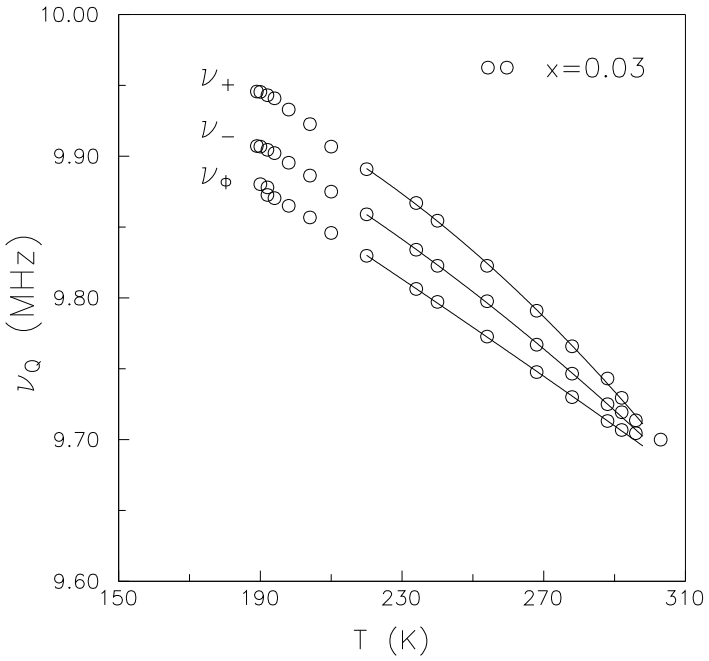

Figure 1. The temperature variation of the singularities in $Rb_2(Zn_{1-x}Cu_x)Cl_4$; for $x = 0.03$.

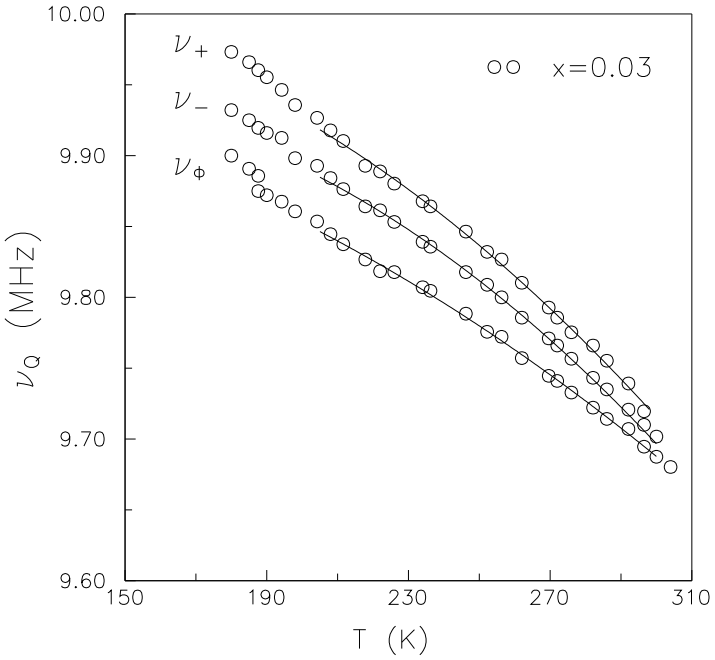

Figure 2. The temperature variation of the singularities in $Rb_2(Zn_{1-x}Cd_x)Cl_4$; for $x = 0.03$.

remains the same. A few degrees above T_C a fourth singularity line, the intensity of which increases with decreasing temperature, is observed, while the intensities of the other three lines

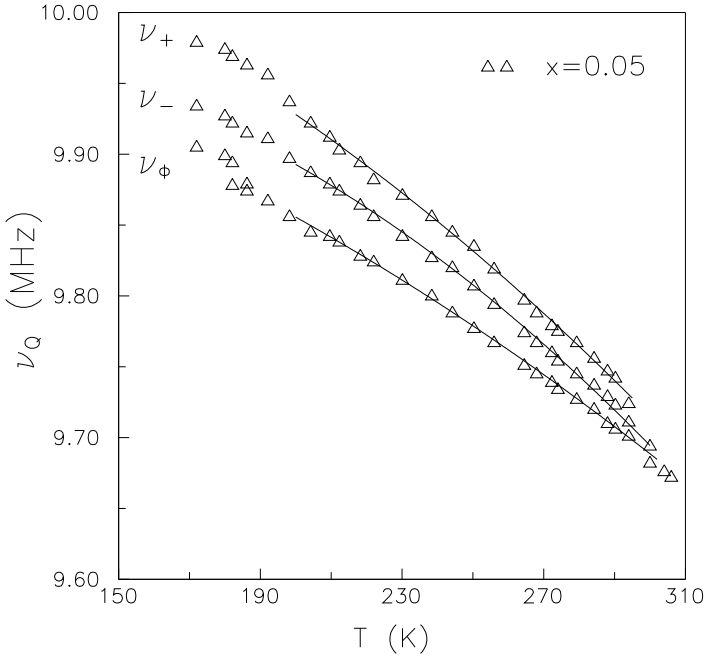

Figure 3. The temperature variation of the singularities in $Rb_2(Zn_{1-x}Cd_x)Cl_4$; for $x = 0.05$.

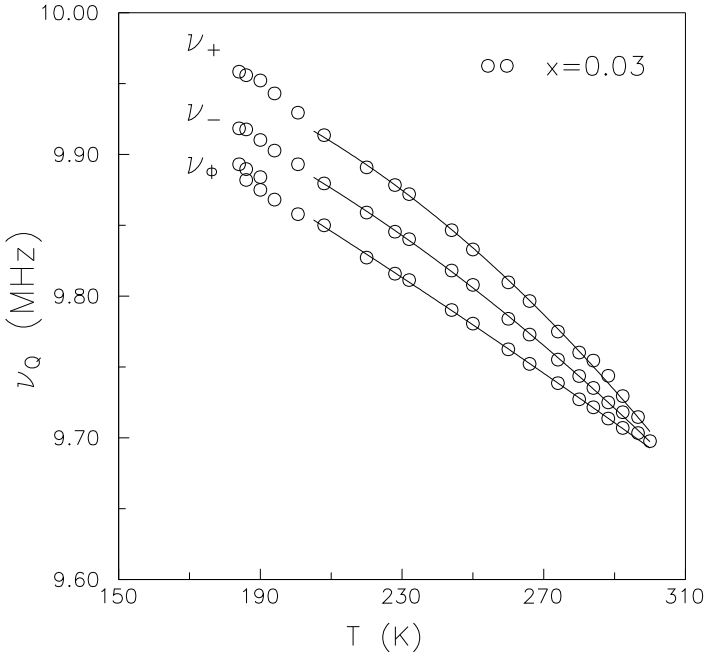

Figure 4. The temperature variation of the singularities in $Rb_2(Zn_{1-x}Hg_x)Cl_4$; for $x = 0.03$.

start decreasing. The observation of this additional singularity indicates the formation of the multi-soliton lattice. The lock-in transition, T_C, is characterized by the disappearance of the

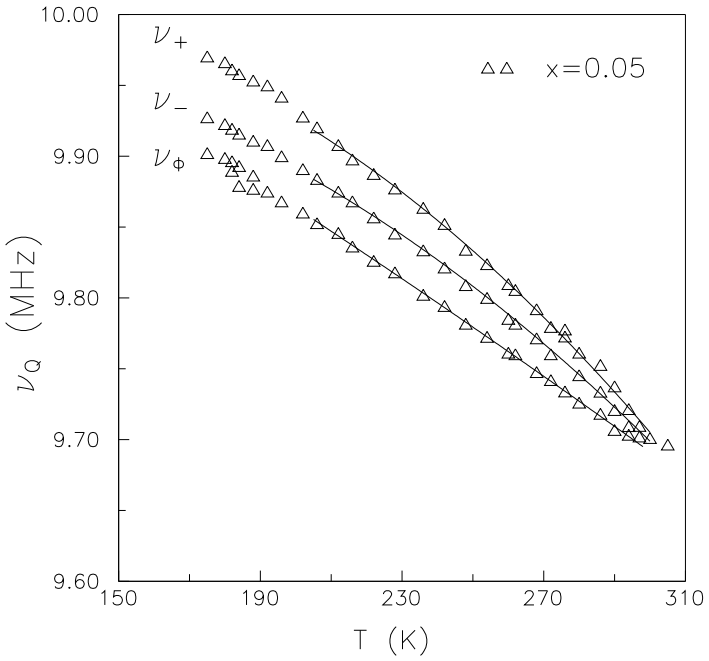

Figure 5. The temperature variation of the singularities in $Rb_2(Zn_{1-x}Hg_x)Cl_4$; for $x = 0.05$.

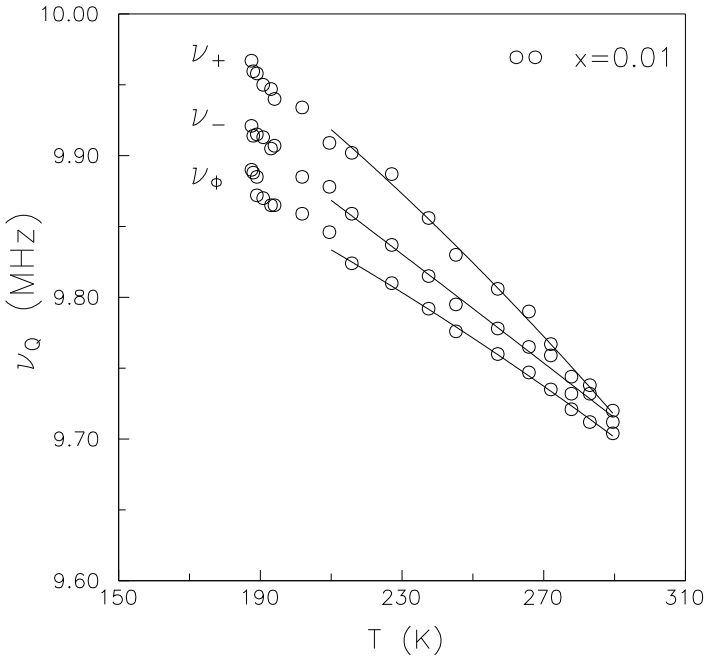

Figure 6. The temperature variation of the singularities in $Rb_2Zn(Cl_{1-x}Br_x)_4$; for $x = 0.01$.

ν_ϕ-singularity and a jump in the value of $T_{1\phi}$ (see figures 8–11). The number of lines observed in the low-temperature commensurate phase is again three. The transition temperatures T_C,

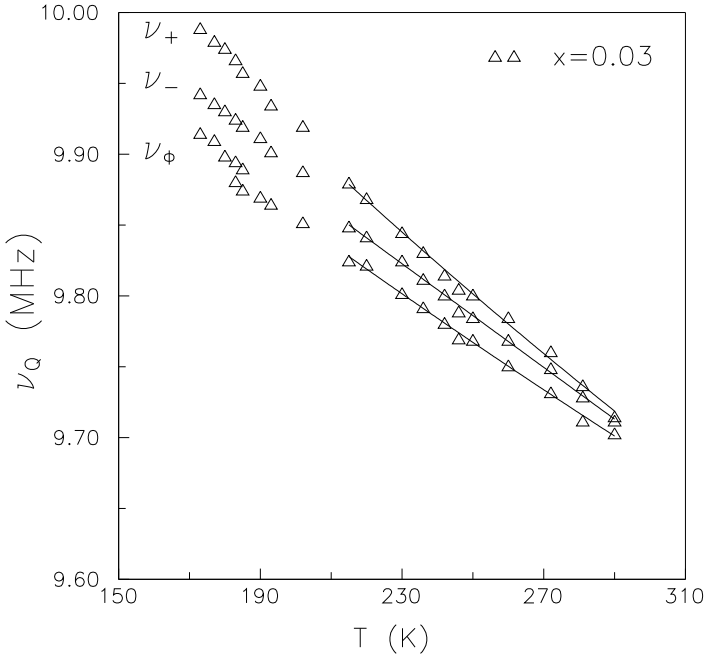

Figure 7. The temperature variation of the singularities in $Rb_2Zn(Cl_{1-x}Br_x)_4$; for $x = 0.03$.

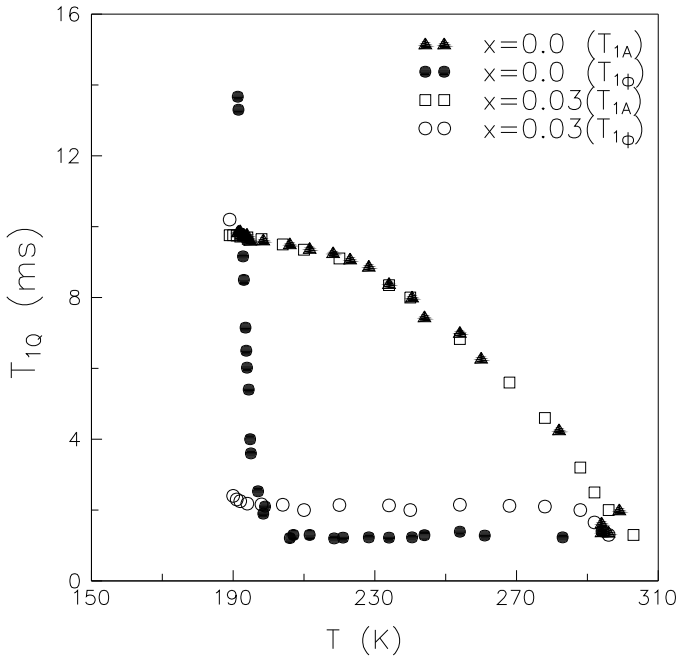

Figure 8. The temperature dependence of the spin–lattice relaxation time T_{1Q} in the IC phase of Rb_2ZnCl_4 and $Rb_2(Zn_{1-x}Cu_x)Cl_4$ with $x = 0.03$.

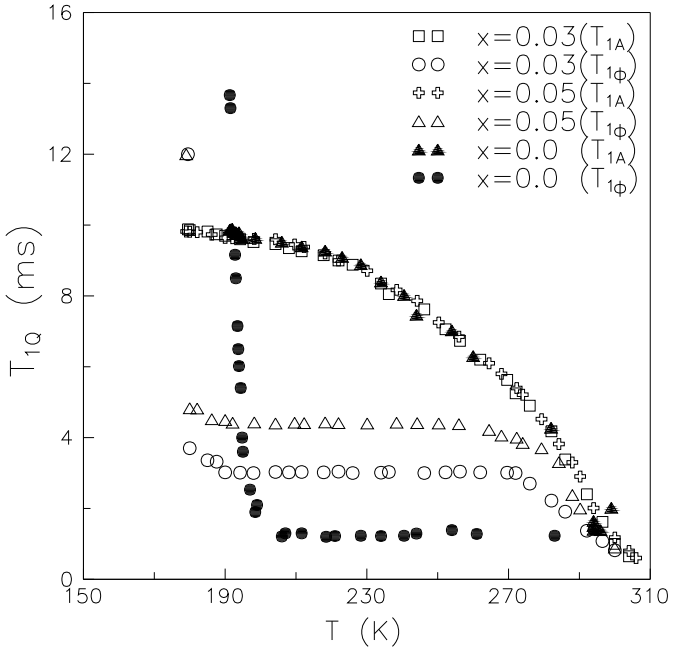

Figure 9. The temperature dependence of the spin–lattice relaxation time T_{1Q} in the IC phase of Rb_2ZnCl_4 and $Rb_2(Zn_{1-x}Cd_x)Cl_4$ with $x = 0.03$ and $x = 0.05$.

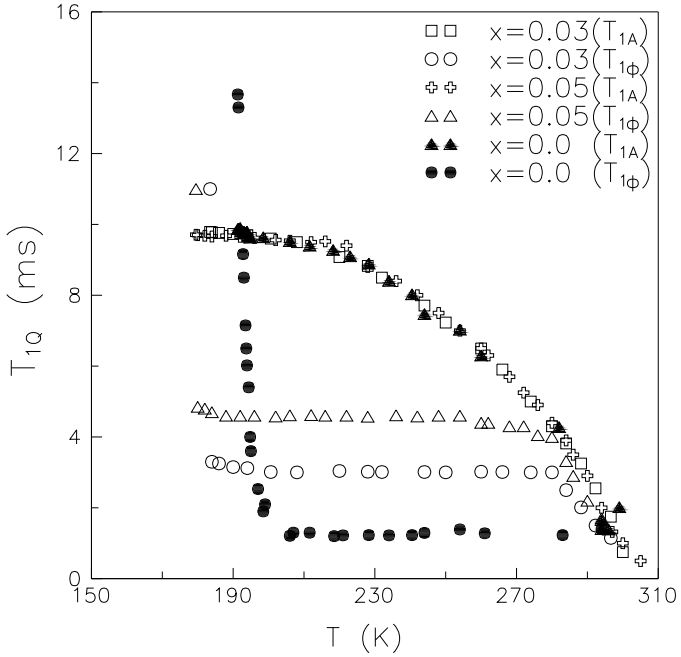

Figure 10. The temperature dependence of the spin–lattice relaxation time T_{1Q} in the IC phase of Rb_2ZnCl_4 and $Rb_2(Zn_{1-x}Hg_x)Cl_4$ with $x = 0.03$ and $x = 0.05$.

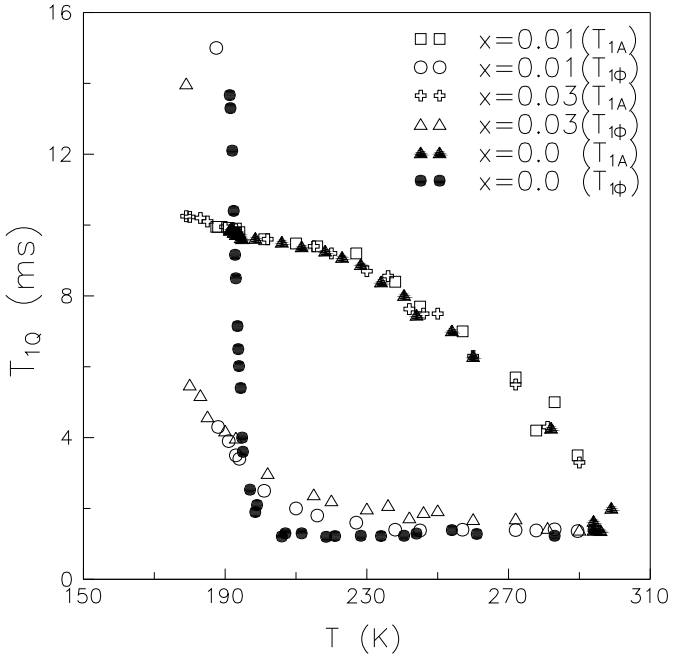

Figure 11. The temperature dependence of the spin–lattice relaxation time T_{1Q} in the IC phase of Rb_2ZnCl_4 and $Rb_2Zn(Cl_{1-x}Br_x)_4$ with $x = 0.01$ and $x = 0.03$.

which are approximately the temperatures where $T_{1\phi}$ starts increasing steeply, are given in table 1. The variations of T_{1A} and $T_{1\phi}$ in $Rb_2(Zn_{1-x}B_x)Cl_4$ (B ≡ Cu for $x = 0.03$, Cd for $x = 0.03$ and 0.05 and Hg for $x = 0.03$ and 0.05) and in $Rb_2Zn(Cl_{1-x}Br_x)_4$ for $x = 0.01$ and 0.03 are shown in figures 8 to 11, respectively. The phason gaps (Δ_ϕ) in these compounds have been estimated from equations (12), (13) and (14). The variations of Δ_ϕ with temperature for the above compounds are shown in figures 12 to 15, respectively. Close to T_C the plane-wave model breaks down and an observed steep increase in $T_{1\phi}$ indicates the formation of the multi-soliton lattice. The increase in $T_{1\phi}$ and its temperature dependence is associated with the splitting of the phason spectrum into an acoustic-like mode ($q < a$, where q is the wave vector associated with the modulation wave and a the width of the commensurate domain) and an optic-like ($q > a$) mode [1, 16]. As the commensurate regions become large (with increasing inter-soliton distance), the contributions to $T_{1\phi}$ from the optic-like mode increase and, at the transition T_C, the contribution from the acoustic-like phason branch becomes zero. At T_C, the values of the phason gap $\Delta_{\phi c}$ for all of the compounds are given in table 1.

5. Discussion

5.1. The role of impurities in the dynamics of the incommensurate phase

The influence of defects and thermal fluctuations on the dynamics of the incommensurate modulation wave near T_C was studied earlier and the deviations from the Landau theory were explained in terms of an intermediate defect-dominated phase described with a model of random internal fields [20]. The transition at T_C in the constant-amplitude approximation (CAA) is a continuous one but may become discontinuous if amplitude variations are taken

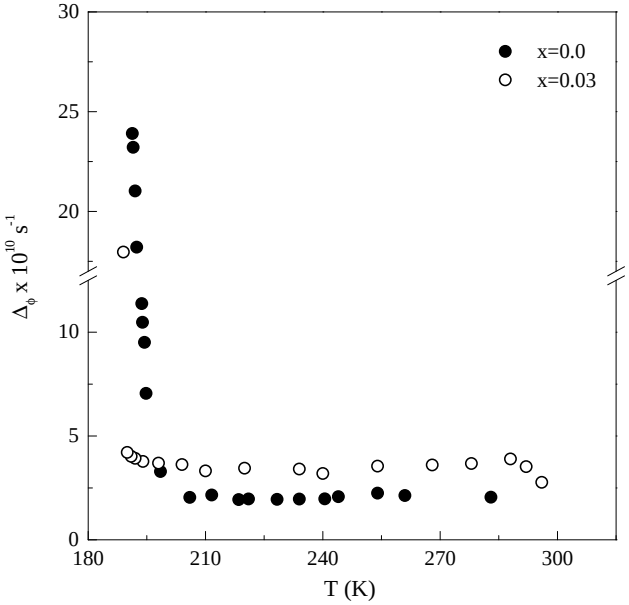

Figure 12. The temperature dependence of the phason gap in the IC phase of Rb_2ZnCl_4 ($x = 0.0$) and $Rb_2(Zn_{1-x}Cu_x)Cl_4$; for $x = 0.03$.

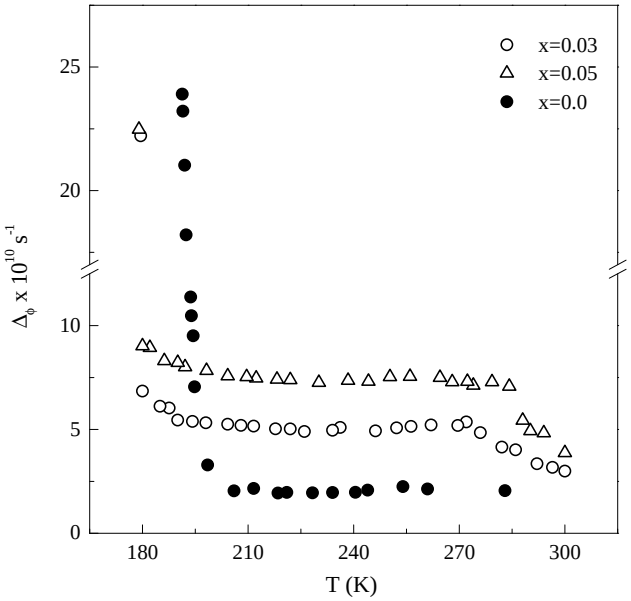

Figure 13. The temperature dependence of the phason gap in the IC phase of Rb_2ZnCl_4 ($x = 0.0$) and $Rb_2(Zn_{1-x}Cd_x)Cl_4$; for $x = 0.03$ and $x = 0.05$.

into account [21]. Close to T_C, the discreteness of the lattice becomes important and may induce a regime of chaotic states [22]. Also a number of experiments [23–26] show that T_C is strongly influenced by the presence of impurities. Thermal fluctuations also strongly influence the impurity pinning effects [27–29] by substantially reducing the pinning energy.

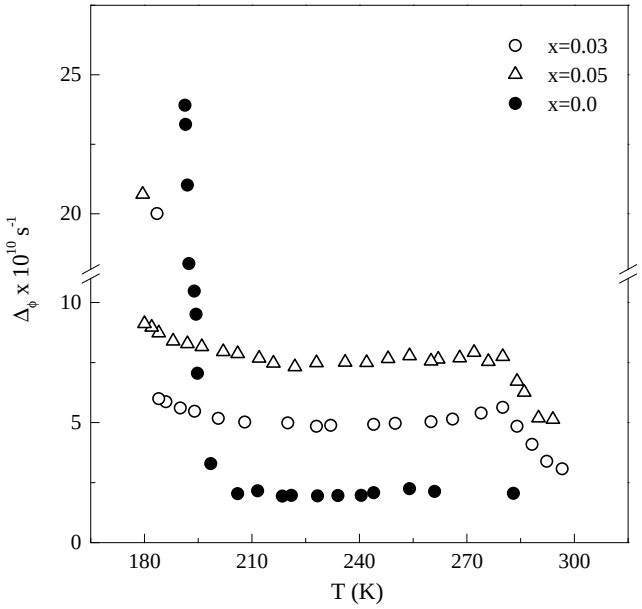

Figure 14. The temperature dependence of the phason gap in the IC phase of Rb_2ZnCl_4 ($x = 0.0$) and $Rb_2(Zn_{1-x}Hg_x)Cl_4$; for $x = 0.03$ and $x = 0.05$.

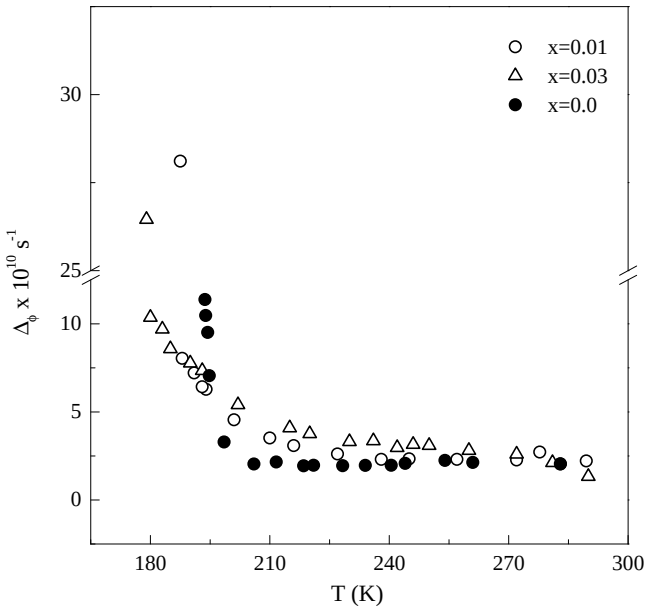

Figure 15. The temperature dependence of the phason gap in the IC phase of Rb_2ZnCl_4 ($x = 0.0$) and $Rb_2Zn(Cl_{1-x}Br_x)_4$; for $x = 0.01$ and $x = 0.03$.

Before reaching T_C from above, the system will enter the region where the incommensurate structure is dominated by defects. The transition from one chaotic state to another takes place when the discommensuration pinning energy (per unit surface) becomes comparable

to the strength of the discommensuration interaction. Below this transition temperature the discommensurations will be pinned at random by the impurities. Characteristic of this intermediate defect-dominated chaotic phase, which can extend well below T_C, is the existence of metastable states [22].

An elaborate and comprehensive review of the theoretical models concerning the influence of impurities in incommensurate systems is given by Prelovsek [4]. Theoretical results concerning the destruction of long-range incommensurate order, the influence of impurities on the low-frequency dynamics and on the lock-in transition, as well as hysteresis effects induced by impurities were discussed. The free-energy density functional f_1 can be generalized for a mixed system by adding a kinetic energy term [11]. The complex order parameter $Q = A\exp(\mathrm{i}\phi)$ is assumed to vary only in the phase ϕ, so the change in the energy density, Δf_1, in the constant-amplitude approximation can be expressed as [11]

$$\Delta f_1 = -\delta A\frac{\partial\phi}{\partial x} + \frac{1}{2}\kappa A^2\,|\nabla\phi|^2 - \gamma A^n\cos(n\phi) - \frac{1}{2}\mu A^2\dot{\phi}^2 \tag{15}$$

where A is the amplitude and ϕ is the phase of the incommensurate modulation wave; n is the symmetry index, μ the effective density of phase oscillations, δ the Lifshitz parameter, κ the elastic constant and γ the anisotropy parameter. In the above equation the Lifshitz term drives the incommensurate modulation at $T = T_I$, while the anisotropy term induces a lock-in transition at $T = T_C$. The elastic term is assumed to be isotropic. Quenched disorder or frozen impurities can be classified according to their symmetry properties relative to the reference commensurate phase. Only defects which couple to the phase ϕ of the incommensurate modulation wave are important [4].

Random-field impurities will act as random fields on the commensurate order parameter discriminating among the n possible commensurate domains with phases ϕ_l where $\phi_l = 2\phi l/n$ $(l = 1, n)$ for $\gamma > 0$. They can be realized by coupling to the order parameter as Q^m, $m < n$. *Random interactions*, also referred to as *random potentials*, do not break the symmetry of the functional, i.e., they do not discriminate among the different commensurate domains but change the anisotropy strength $\gamma \to \gamma + \Delta\gamma$ locally [4]. Impurities which locally change the elastic constant κ and couple to the phase derivative also fall into this category. In the case of *random-potential*-type impurities, the phase deviation from the plane-wave solution induced at any point r by stationary impurities $\psi = \phi - qr$ is determined by the functional where the change in the energy density is given by

$$\Delta f = \frac{1}{2}\kappa A^2\,|\nabla\psi|^2 - \Delta\gamma\, A^n\cos[n(qr+\psi)] \qquad |q| = \kappa/\delta. \tag{16}$$

In the weak-pinning regime, ψ cannot adjust itself maximally to the impurity separately because of the strong elastic term restricting variations in ψ. Adjustments will take place on a larger scale, over a domain size L_0 within which $|\Delta\psi| < \pi/m$. In the strong-pinning limit the potential term is locally optimized, so for each impurity site at r, $q_0 r + \psi(r_i) \approx 2\pi k/m$. For the weak-pinning case, assuming that $\Delta\gamma = \Delta\gamma_0$ in the vicinity $(R < R_0)$ of the defect and $\Delta\gamma = 0$ for $R > R_0$, the average distance between defects L_0 is much larger than R_0, i.e. $L_0 = (n_i)^{-1/3} \gg R_0$ with n_i being the defect ion concentration. Within, the defect range $(R < R_0)$ we have $\psi = \psi_0$, whereas $\psi = \psi_0 R_0/R$ for $R > R_0$. For $\Delta\gamma/\gamma < 1$, the phase deviation induced by the defect remains small, $\psi_0 < \pi/n$ (for the symmetry-non-breaking impurity where $m = n$) over the whole incommensurate phase. With this *ansatz* the free-energy difference per defect, from equation (15), becomes

$$\Delta F = \frac{1}{2}\kappa A^2 R_0\, 2\pi\psi_0^2 + nA^n\,\Delta\gamma_0\, V_0\sin(nqr)\psi_0 \tag{17}$$

where $V_0 = 4\pi R_0^3/3$. The temperature dependence of the phason gap induced by an impurity with symmetry m characterizing it as either *random-field* or *random-interaction* type is given by [4]

$$\Delta_\phi \propto (T_\mathrm{I} - T)^{\beta(m-2)} \tag{18}$$

($m = n = 6$ for the symmetry-non-breaking impurity, as in pure Rb_2ZnCl_4). On the other hand, for a strong *random-field*-like pinning by the defect, $L_0 \approx (1/n_i)^{1/3}$, so the gap is $\Delta_\phi \approx c\pi/L_0 = (\kappa/\mu)^{1/2}\pi n_i^{1/3}$ where c is the phason velocity, independent of temperature. Thus it is seen that the symmetry parameter m characterizing the impurity can characterize the defect as symmetry non-breaking or otherwise and has been found by fitting the data near T_I to equation (18) wherein a constant term is added to Δ_ϕ in equation (18) to account for the contributions to the phason gap arising from discrete-lattice effects and defects present even in the pure system (for Rb_2ZnCl_4, $m = 6$).

The influence of phase fluctuations of the modulation wave on the NQR line shape can be evaluated using certain simplified models for the motions of the modulation wave. A reasonable model [30] is that in which the phase fluctuations are represented by standing waves within an average coherence volume V_C. In the strong-pinning regime, where the phase of the modulation wave between pinning centres can fluctuate freely, $V_C = 1/n_i$, n_i being the impurity concentration. Then V_C is independent of temperature and hence Δ_ϕ and consequently $T_{1\phi}$ are independent of temperature. In the weak-pinning regime, the system is assumed to separate into domains [31]. Within each of these domains, the impurity-induced phase distortion varies slowly and takes random values in different domains. The phase of the modulation wave is fluctuating freely within each domain and the coherence volume V_C is identified with the domain volume. In this case, V_C is temperature dependent [30] and hence $T_{1\phi}$, through Δ_ϕ and its temperature dependence, will be given by equation (18). Close to T_I, even in the case of impurities that have strong-pinning natures, the order parameter of the incommensurate phase itself will be very small. As such, the coherence volume becomes temperature dependent, signalling the onset of the weak-pinning regime. Under these assumptions, the symmetry parameter (m) has be evaluated as in the weak-pinning case using equation (18).

5.2. Defect pinning at the metal site in Rb_2ZnCl_4

The temperature dependence of the observed singularities (ν_+, ν_- and ν_ϕ) in all of the compounds with doping of Cu, Cd or Hg at the metal (Zn) site in Rb_2ZnCl_4 gave β-values identical to that for the pure system, as seen from table 1. This shows that the singularities in these systems develop similarly to that in the pure system. It is seen from figures 8–10 that doping with Cu (smaller than Zn), Cd or Hg (both of which are bigger than Zn) leads to an increase of $T_{1\phi}$ and hence an enhancement of Δ_ϕ (increasing with increase in the concentration of the dopant). It is also seen that $T_{1\phi}$, which rises sharply within the few degrees below T_I, is independent of temperature thereafter throughout the incommensurate phase. It picks up a temperature dependence only very close to the lock-in transition temperature T_C. T_{1A}, on the other hand, follows a very similar critical temperature dependence to that for pure Rb_2ZnCl_4. As discussed earlier, such a temperature-independent $T_{1\phi}$ (observed with Cu, Cd or Hg doping at the Zn site) is indicative of the strong-pinning nature of the substituted impurity. This could be visualized as follows: between the pinning centres the phase fluctuations fluctuate freely and can be represented by standing waves within an average coherence volume. And this coherence volume is independent of temperature, leading to a temperature-independent Δ_ϕ and consequently $T_{1\phi}$. The increases in Δ_ϕ due to Cu, Cd or Hg doping from that for pure

Rb_2ZnCl_4 are shown in figures 12–14 respectively. As seen from figures 12 and 13 (Cd or Hg doping), Δ_ϕ increases with increasing concentration but remains temperature independent throughout the incommensurate phase. Thus it appears that this evidence of strong pinning is site specific, as both smaller (Cu) and bigger (Cd and Hg) ions (compared to Zn) substituted at the metal site lead to such an effect. The values of the phason gap, $\Delta_{\phi c}$, for different concentrations of the dopants are given in table 1.

It has been observed that substitution at the metal site enhanced T_I [26] and suppressed the lock-in transition T_C considerably. It is seen from table 1 that 3% Cu suppressed T_C to 190 K and 3% Hg suppressed it to 184 K (from 192 K for pure Rb_2ZnCl_4). This shows that the effect of suppression of T_C is enhanced with increase in the size of the dopant (from Cu to Hg). Also, for a given dopant, an increase in its concentration suppresses T_C further. The value of the symmetry parameter (m) estimated from equation (18) for the Cu impurity has been found to be 5, and that for Cd and Hg is $m = 4$, indicating that Cu, Cd and Hg are *random-field*-type impurities breaking the symmetry of the host Rb_2ZnCl_4 and that they provide strong pinning of the incommensurate modulation wave. A typical fit of the data to equation (18) for a 3% Cd doping at the Zn site is shown in figure 16.

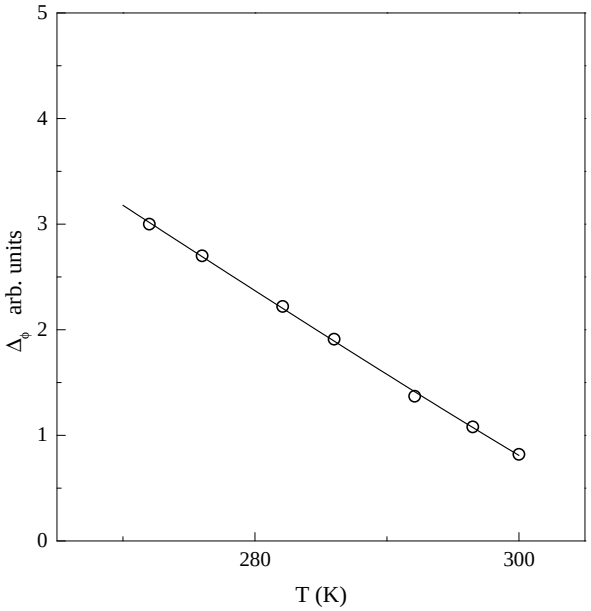

Figure 16. The best fit (solid curve) to the experimental data (symbols) used in evaluating the symmetry parameter $m = 4$ for $Rb_2(Zn_{1-x}Cd_x)Cl_4$; for $x = 0.03$.

5.3. Defect pinning at the halogen site in Rb_2ZnCl_4

The three singularities (ν_+, ν_- and ν_ϕ) observed with Br doping at the halogen site in $Rb_2Zn(Cl_{1-x}Br_x)_4$ vary with temperature to give β-values similar to that for the pure system (table 1). It is seen from figure 11 that doping with Br leads to an increase of $T_{1\phi}$ and hence implies an enhancement of Δ_ϕ (increasing with increase in the concentration of the dopant). It is also seen that $T_{1\phi}$ increases slowly starting from T_I, and is temperature dependent throughout the incommensurate phase. Its temperature dependence increases close to the lock-in transition temperature T_C. T_{1A}, on the other hand, follows the same temperature dependence as for pure

Rb_2ZnCl_4. This variation of $T_{1\phi}$ is indicative of the weak-pinning nature of the substituted impurity unlike the case for the metal site substitutions. The variation of Δ_ϕ due to 1% and 3% Br doping relative to pure Rb_2ZnCl_4 is shown in figure 15. It is seen that Δ_ϕ increases with increasing concentration and is temperature dependent throughout the incommensurate phase.

Substitution at the halogen site suppresses T_I [26] unlike metal site substitution. It also suppressed the lock-in transition T_C. It is seen from table 1 that 1% Br impurity suppressed T_C to 188 K and 3% Br suppressed it to 180 K (from 192 K for pure Rb_2ZnCl_4), showing that the effect of the suppression of T_C is enhanced with increase in the size of the anion (from Cl to Br). Also, increase in the concentration of the Br suppresses T_C further. $\Delta_{\phi c}$ values for different concentrations of Br are given in table 1. The value of the symmetry parameter (m) estimated from equation (18) for the Br impurity has been found to be $m = 6$, indicating that Br is a random-potential-type impurity and does not break the symmetry of the host Rb_2ZnCl_4. A fit for the estimation of $m = 6$ from equation (18) for a 1% Br doping at the Cl site is shown in figure 17.

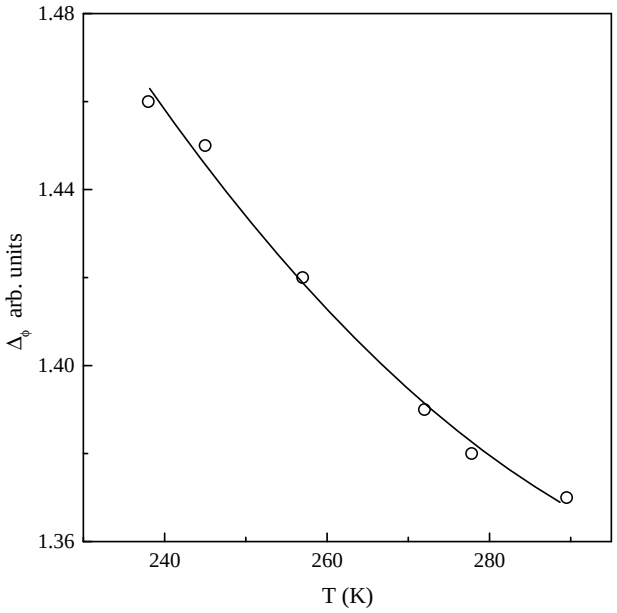

Figure 17. The best fit (solid curve) to the experimental data (symbols) used in evaluating the symmetry parameter $m = 6$ for $Rb_2Zn(Cl_{1-x}Br_x)_4$; for $x = 0.01$.

6. Conclusions

(a) Doping at the metal site (with Cu, Cd or Hg) induced strong pinning of the incommensurate modulation wave irrespective of the size of the dopant. This probably is the first such observation with NQR, and strong pinning seems to be site specific at the Zn site.

(b) Substitution of Br at the halogen site has somewhat different effects on T_I and T_C compared to substitution of other impurities. This suppressed both T_I and T_C, unlike the effect of doping at the Zn site (T_C suppressed and T_I enhanced) or at the Rb site (only suppression of T_I).

(c) The present study permits a characterization of the various impurities in terms of their symmetry parameter (*random-field* or *random-potential* type) as well as the nature of the pinning (strong or weak).

Acknowledgments

One of the authors (UMS) gratefully acknowledges financial support from the University Grants Commission, India, in the form of a research fellowship. This work was supported in part by the Office of Naval Research (Grant No N00014-97-1-0994) under the Indo-US joint research project.

References

[1] Blinc R, Prelovsek P, Rutar V, Seliger J and Zumer S 1986 *Incommensurate Phases in Dielectrics* vol 1, ed R Blinc and A P Levanyuk (Amsterdam: North-Holland) p 143
[2] MacMillan W L 1976 *Phys. Rev.* B **14** 1496
[3] Bak P and Pokrovsky V L 1981 *Phys. Rev. Lett.* **47** 958
[4] Prelovsek P 1988 *Phase Transitions* **11** 203
[5] Hamano K, Ema K and Hirotsu S 1981 *Ferroelectrics* **36** 343
[6] Subramanian R K, Venu K and Sastry V S S 1994 *J. Phys.: Condens. Matter* **6** 2377
[7] Milia F, Papavassiliou G and Ginnakopoulos E 1989 *Z. Naturf.* a **45** 323
[8] Milia F, Papavassiliou G and Ginnakopoulos E 1989 *Phys. Rev.* B **39** 12 349
[9] Milia F and Papavassiliou G 1990 *Geometry and Thermodynamics* ed J C Toledano (New York: Plenum) p 429
[10] Subramanian R K, Venu K and Sastry V S S 1995 *J. Phys.: Condens. Matter* **7** 3033
[11] Blinc R, Dolinsek J, Prelovsek P and Hamano K 1986 *Phys. Rev. Lett.* **56** 2387
[12] Rene P, Michel J, Lucien G and Genevieve G 1990 *Ferroelectrics* **107** 229
[13] Etxebarria I, Perez-Mato J M and Criado A 1990 *Phys. Rev.* B **46** 2746
[14] Subramanian R K, Uma Maheswari S, Venu K and Sastry V S S 1996 *Z. Naturf.* a **51** 745
[15] Alexandrova I P 1986 *Incommensurate Phases in Dielectrics* vol 1, ed R Blinc and A Levanyuk (Amsterdam: North-Holland) p 277
[16] Blinc R 1981 *Phys. Rep.* **79** 331
[17] Zumer S and Blinc R 1981 *J. Phys. C: Solid State Phys.* **14** 465
[18] Peltzelt 1981 *Phase Transitions* **2** 155
[19] Zeyen C M E 1983 *Physica* B **120** 283
[20] Prelovsek P and Blinc R 1984 *J. Phys.: Solid State Phys.* **17** 577
[21] Prelovsek P 1982 *J. Phys.: Solid State Phys.* **15** L269
[22] Bak P 1982 *Rep. Prog. Phys.* **45** 587
[23] Hamano K 1986 *Incommensurate Phases in Dielectrics* vol 1, ed R Blinc and A P Levanyuk (Amsterdam: North-Holland) p 365
[24] Mashiyama H, Tanisaki S and Hamano K 1982 *J. Phys. Soc. Japan* **51** 2538
[25] Blinc R, Apih T, Dolinsek J, Prelovsek P, Slak J, Ailion D C and Ganesan K 1994 *Phy. Rev.* B **50** 2827
[26] Uma Maheswari S, Venu K and Sastry V S S 1999 to be published
[27] Rice T M, Whitehouse S and Littlewood P 1981 *Phys. Rev.* B **24** 2571
[28] Fajdiga A M, Apih T, Dolinsek J, Blinc R, Levanyuk A P, Minyukov S A and Ailion D C 1992 *Phys. Rev. Lett.* **69** 2721
[29] Dolinsek J, Fajdiga A M, Apih T, Blinc R and Ailion D C 1994 *Phys. Rev.* B **50** 9729
[30] Papavassiliou S, Angnostopoulos A and Milia F 1993 *J. Phys.: Condens. Matter* **5** 9295
[31] Fukuyama H and Lee P A 1978 *Phys. Rev.* B **17** 535